Silicon (2024) 16:3233–3241
https://doi.org/10.1007/s12633-024-02883-3

RESEARCH

Investigation of Sintering Behavior of Sol Gel Derived SiO_2-Al_2O_3-B_2O_3 Glasses

Sara Ahmadi[1] · **Bijan Eftekhari Yekta**[2]

Received: 1 December 2023 / Accepted: 30 January 2024 / Published online: 22 February 2024
© The Author(s), under exclusive licence to Springer Nature B.V. 2024

Abstract

Synthesizing of alumino-borosilicate glasses in the SiO_2-B_2O_3-Al_2O_3 system using the sol–gel method was considered. Transparent and dense glasses were obtained by various heat treatment programs applied on the dried gels. The process of converting the gel to glass involves complex transformations including both structural and chemical changes. Consequently, investigating the sintering behavior of these synthesized powder holds significant academic merit. In order to achieve this objective, the density of monolithic glass was assessed subsequent to sintering at various temperatures. Besides, the sintering activation energy of glasses in both isothermal and non-isothermal circumstances was estimated. The relative density values for various sintered glass compositions were between 96.5- 99.6%. The sintering activation energy under isothermal condition for glasses exhibited an increase with increasing of aluminum oxide amounts from 237 up to 314 kJ/mol. Furthermore, the results showed that crystallization of the sample can increase its sintering activation energy up to 414 kJ/mol. Under non-isothermal condition and for different heating rate for the samples, the sintering activation energy values for glass which had the lowest content of Al_2O_3 was the same. However, in the composition with the highest content of ZnO, its linear shrinkage increment indicated a significant decrease in its sintering activation energy despite the crystallization of the mullite phase within the glass.

Keywords Sol gel · Sintering behavior · Crystallization · Hot stage microscopy

1 Introduction

The sol–gel process is widely employed for synthesizing of various powders and glassy materials as well. The sol–gel process is predicated upon the chemical interaction between colloidal particles present in a sol or polymeric entities dissolved in a solution, resulting in the formation of a gel. An amorphous and dense material can be obtained after the sintering the dried and porous gel. In this particular pathway, the requisite glass is achieved at a significantly reduced temperature compared to the temperature required for melting a similar composition [1]. This approach is appropriate for systems that necessitate elevated temperatures for melting or in cases where achieving homogeneity is challenging due to the notably high viscosity of the molten substance. The utilization of a chemical approach becomes imperative, particularly in cases when the evaporation points of the various oxides differ, since it is the sole means of averting the loss of certain constituents. By employing this particular approach, the uniformity is achieved at the molecular scale, hence enabling the production of glasses by elevated levels of purity with high variety of compositions.

The ultimate configuration of the dried gel is dependent upon its initial. The dried gel consists of interconnected agglomerates including primary particles, exhibiting varying sizes of both open and closed pores. The particles are coated with hydroxyl (OH) and alkoxy (OR) groups, which necessitate their removal during the process of gel to glass conversion [1–3]. The structural configuration of dried gel exhibits similarities to that of glass; but, with a lower density in comparison. During the heat treatment process, the gel experiences an increase in density and undergoes a structural transformation, resembling that of molten glass. The

✉ Sara Ahmadi
s.ahmadi@standard.ac.ir

[1] Construction and Minerals Research Group, Technology and Engineering Research Center, Standard Research Institute, Alborz, Iran

[2] Ceramic Division, School of Materials and Metallurgy Engineering, Iran University of Science and Technology, Tehran, Iran

particles are interconnected and the pores are fully eliminated. The underlying mechanism responsible for this process involves diffusion and viscous flow. The conversion of a gel substance into glass involves a multifaceted process characterized by numerous structural and chemical alterations. According to reports, the phase transition from gel to glass involves at least four mechanisms including capillary contraction, condensation and polymerization, structural relaxation, and viscous flow. The temperature at which each of these mechanisms is dominant depends on the size of the pores, the skeletal density of the gel, the heating rate and the thermal history of the gel [4].

During the earliest stages of the thermal process, the primary factor contributing to gel contraction is capillary contraction. This phenomenon is closely linked to significant weight loss and minimal shrinkage. The density of the gel skeleton increases as a result of condensation reactions and the gel undergoes shrinking with increasing temperature. Throughout this procedure, which is associated with further polymerization of the system, the residual OH and OR groups are eliminated as water (H_2O) and alcohol (ROH) [1]. The elimination of these groups results in a reduction in the mass of the gel.

The gel undergoes a process known as structural relaxation when the sintering temperature is raised, resulting in an irreversible transformation. The aforementioned process involves the reconfiguration of chemical bonds and the diffusion of atoms, without the liberation of water or any other substances. This process effectively diminishes the free energy inside the system. Ultimately, once the viscosity of the system decrease sufficiently fast shrinkage occurs as a result of the viscous flow, leading to the closure of the gel pores [2, 5].

While there is no explicit temperature differentiation between the aforementioned processes, it has been documented that the initial temperature at which viscous flow occurs during gel sintering is in proximity to the glass transition temperature observed in molten glasses [6].

In the process of gel to glass conversion, it is imperative to eliminate the organic groups and residual substances prior to pore closure. Typically, the utilization of an oxidizing atmosphere is necessary [7].

A very slow heating rates result in the elimination of hydroxyl groups and a subsequent rise in viscosity. Consequently, the shrinkage process ceases prior to achieving complete densification. Conversely, when subjected to a high heating rate, these materials have a tendency to remain within the structure, leading to their entrapment and subsequent formation of cracks in the glass [5, 8–11].

Despite the increasing usage the sol gel technique in the synthesized of glasses, there are not many systematic researches to understand the gel-to-glass conversion process. In the present work, the sintering mechanism and activation energy as well as the density variations of the monolithic transparent glasses prepared by the sol gel method have been reported.

2 Experimental Procedures

2.1 Starting Materials and Preparation of Hydrogels

The alumino-borosilicate glasses in SiO_2-Al_2O_3-B_2O_3 system were prepared by sol–gel method. The composition of the synthesized glass is given in Table 1. The materials were reagent grade chemicals consisted of tetraethyl orthosilicate TEOS, ($Si(OC_2H_5)_4$, 99% pure), aluminum-sec-butoxide ($Al(OC_4H_9)_3$ 97% pure), trimethyl borate ($B(OCH_3)_3$ 99% pure), barium, zinc and potassium nitrates (99.9% pure).

TEOS diluted in ethanol (1:4 molar ratio) and hydrolyzed using a catalyst of 1M HCl solution. Gradually, trimethyl borate and aqueous solutions of potassium, barium, and zinc nitrates were added. Organic citric acid was utilized as a chelating agent to build a stable combination with aluminum ions (1:1 molar ratios) to increase the uniformity of the sol. A dilute solution of Al-sec-butoxide and isopropanol (1:4 molar ratios) was slowly added to the citric acid aqueous solution. In our previous work [12] it has been explained how employing a chelating agent affects the transparency of the produced sol.

The alkoxide and nitrate solutions were combined with the chelated aluminum solution after 2 h. The solution was agitated for 2 h before being poured into a polypropylene tube. While the tube mouth was closed, gelation occurred within 24 h at room temperature.

The Xerogels were made by slow drying the gels at room temperature. The authors have previously conducted research on the impact of several parameters on the drying process of gels [13]. The xerogels underwent heat treatment

Table 1 The composition of synthesized glasses

Glass composition	SiO_2	B_2O_3	Al_2O_3	BaO	K_2O	ZnO
GI	66	18	7	3	6	0
GII	66	10	15	3	6	0
GIII	48	10	30	6	6	0
GIV	48	10	30	0	2	10

at different temperatures, using a heating rate of 1°C/min in order to produce glass.

2.2 Characterization Techniques

The determination of the bulk density of the specimens was conducted using the Archimedes method subsequent to subjecting them to heat treatment at various temperatures in air atmosphere. The gas pycnometer was employed to determine the powder density of the synthesized glasses.

The crystallinity of the specimens was investigated by X-ray diffractometer (XRD, JEOL JDX 8030). The investigation of the sintering behavior of the produced gels was conducted using simultaneous thermal analysis (STA-1640, Polymer Laboratories, England) and hot stage microscopy (HSM, Misura 2.1 expert). The heating rate was 10 °C/min. In order to achieve the desired objective, the glass powder underwent an initial sintering process at a temperature of 600 °C, followed by subsequent testing. The sintering activation energy of the glass was determined by conducting the test at heating rates of 10, 15, 20, and 25 °C/min.

3 Results and Discussion

3.1 The Sintering Mechanism of Synthesized Glasses

Table 2 presents the true density of the powdered glasses GI, GII, GIII and GIV. Additionally, Fig. 1 illustrates the density variations of synthesized monolithic glasses after heating at various temperature.

It should be noted that the relative densities of GI, GII and GIII glasses were 99.6, 99.5 and 99.3%, respectively,

Table 2 Powder density of synthesized glasses

Glass composition	GI	GII	GIII	GIV
Powder density (g/cm3)	2.25 ± 0.0032	2.45 ± 0.0024	2.52 ± 0.0015	2.6 ± 0.0015

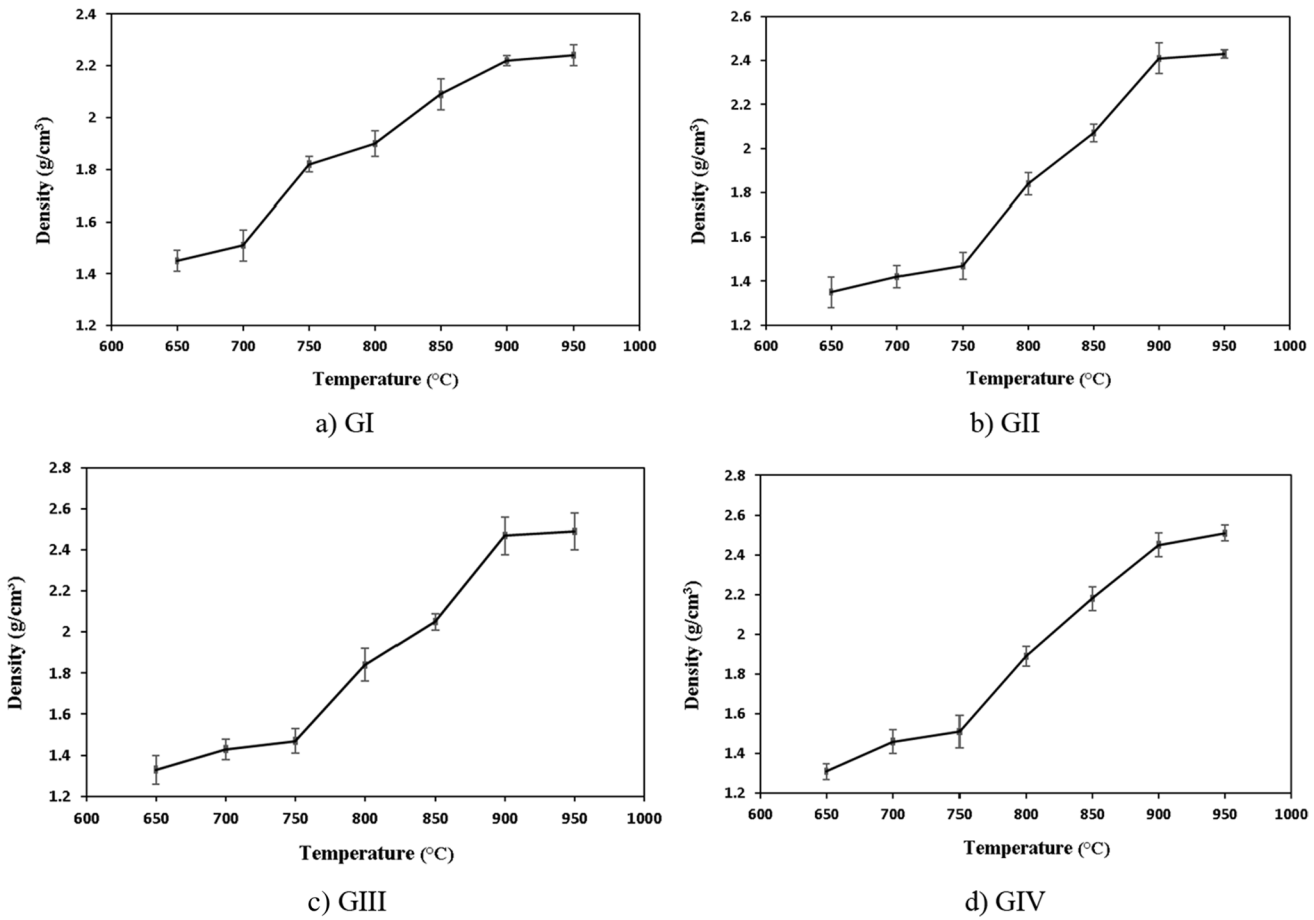

Fig. 1 The bulk density of synthesized glasses after heating at various temperature for 2 h

following the sintering at 950 °C for 2h. Based on the Table 2, it can be observed that the GIV shows the least relative density, i.e. 96.5%, subsequent to undergoing a sintering process at 950°C. Crystallization in GIV is probably responsible for the lower density of it. As it is known the viscosity of the glassy specimen increases with crystallization which can hindered the viscous flow and sintering in it as well.

Figure 2 depicts the sintering curve of the synthesized glasses, using a hot stage microscope(HSM), as well as their weight variations acquired from the thermogravimetry (TG) measurement conducted at a heating rate of 10 °C/min.

Based on the weight variation plot, it is evident that beyond a temperature of 600 °C, no discernible decrease in weight is observed across all synthesized compositions. Hence, it can be concluded that the fluctuations in the sintering curve's height are unrelated to the liberation of volatile compounds, but are dependent on sintering procedure as a result of viscous flow. In the HSM results and in some

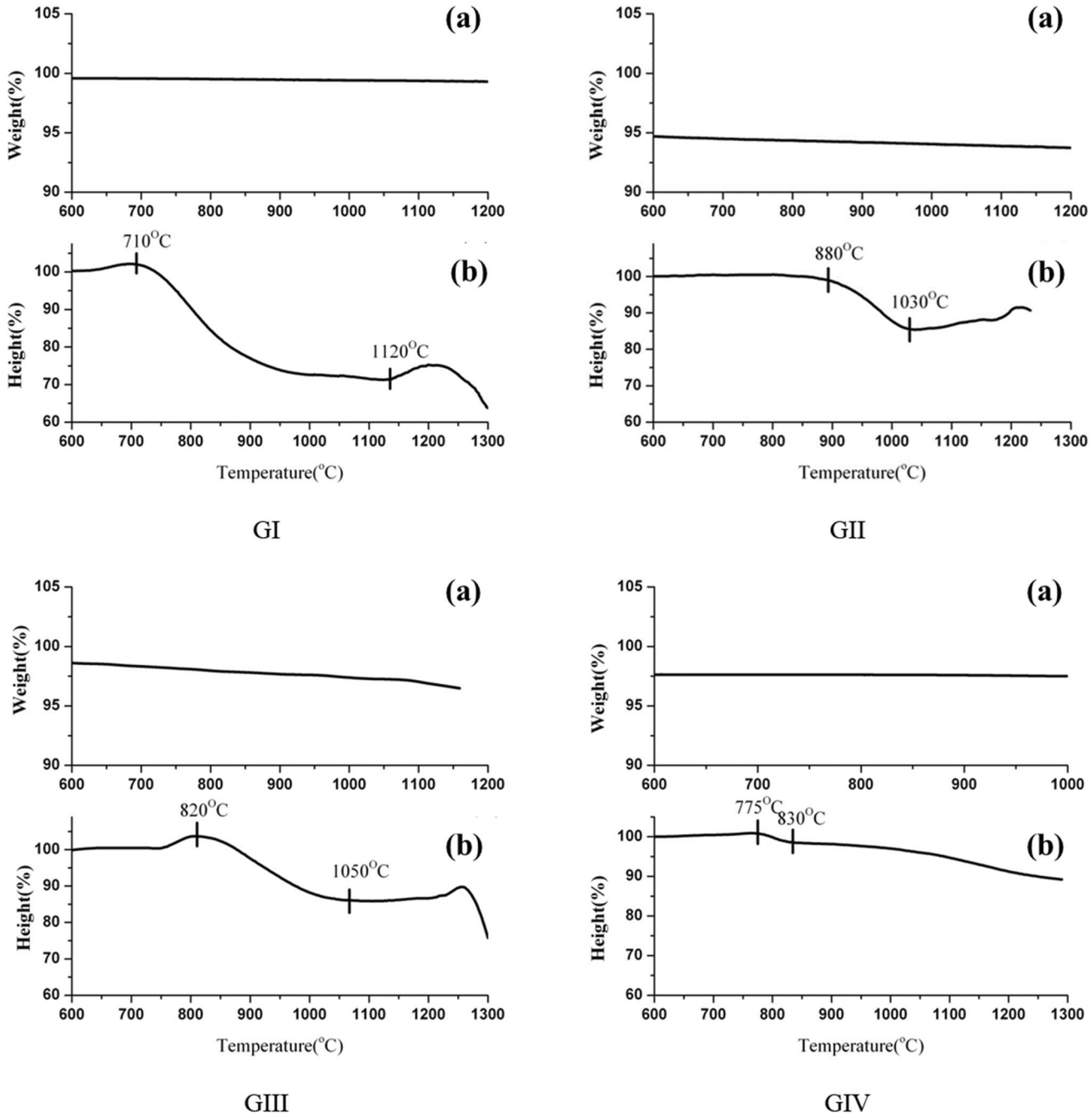

Fig. 2 Variations in (**a**) weight and (**b**) height of synthesized glasses with temperature determined from TG at heating rate of 10°C/min

temperatures an increase in height of the samples is seen which is related to liberation of entrapped air within the particles. Following this step, there is a notable reduction in the vertical dimension of the samples, signifying the onset of viscous flow and an accompanying elevation in the samples' density. The figures also show the region temperature in which viscous flow accelerated in the samples. The viscosity of glasses GI, GII, and GIII is lowered at temperatures 710 °C, 860 °C, and 875 °C, respectively, and the viscous flow mechanism continues up to temperatures of approximately 1120°C, 1030°C and 1050°C. According to the results derived from the density measurement, the GI exhibits a relative density of 99.6% when sintered at 950 °C. The disparity in the ultimate temperature observed in the viscous flow process during thermal tests and density measurements can be attributed to the time-depended nature of the viscous flow process. The soaking time of the samples was 2h at each firing temperature. Consequently, the glass pores underwent sufficient time for closure as a result of the viscous flow process. However, during this time the entrapped air inside the closed pores tends to escaped from it. Such an event leads to the swelling of the glass, the height of the glass sample increases in the HSM. The effect of such an event can be seen in the HSM of the glasses GI, GII and GIII.

Based on the X-ray diffraction (XRD) patterns depicted in Fig. 3, it can be observed that the GI, GII and GIII have an amorphous structure within the specified temperature range. Ultimately, the glass melts completely with increasing the temperature. This behavior shows itself by a significant reduction in the height of the HSM curves.

The above-mentioned swelling mechanism is not seen in sample GIV at its examined region temperature (Fig. 3). It is known that complete densification of a glass, which tends to be crystallized during firing, shifts to higher temperature, due to increasing of its viscosity. This impeding the full closure of the its pores. According to Fig. 3, mullite has crystallized in the GIV sample after firing at temperature 950 °C. The resulted sample showed an approximately 3.5% porosity. The sintering curve of the GIV exhibits a consistent decline in height, suggesting that despite the rising of sintering temperature its sintering has remained incomplete.

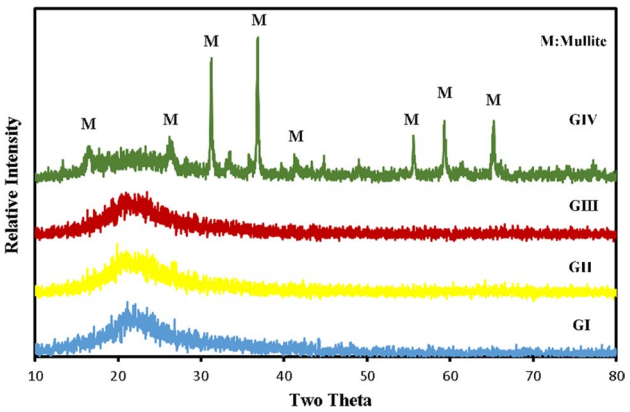

Fig. 3 XRD patterns of glasses after sintering at 950 °C for 2h

It is known that when non-sinterable particles added to a sinterable matrix, the dissimilarity between the sintering rates of the two phases develops tangential tensile stresses in the matrix phase and isostatic compressive stresses in the second phase during firing [14]. By generalizing this phenomenon to the current research work, it can be said that the formation of mullite in the GIV caused the loss of sintering of this sample during firing.

3.2 The Activation Energy of Sintering Under Isothermal Condition

Brinker et al. demonstrated the potential value of employing contraction equations at a constant heating rate, which are independent of a particular model, for the purpose of forecasting the behavior of gel compaction [15].

To investigate the sintering characteristics of the synthesized glasses, the sintering activation energy of the glasses was determined using the Kingery's equation under isothermal conditions [16]:

$$(\Delta L/L_0)^n = Kt/T \quad (1)$$

where $\Delta L/L_0$ is the linear shrinkage after firing for time t, n is the power, K is the temperature-dependent rate constant, and T is the absolute temperature. Correspondingly, the rate constant K within a limited temperature range can be mathematically described by the Arrhenius relation as follows:

$$K = K_0 \exp(-E/RT) \quad (2)$$

where E is the activation energy of viscous flow, K_0 is a constant and R is the gas constant.

In order to achieve the intended objective, the synthesized monolithic glasses underwent a sintering process at temperatures 875, 900, 925, and 950 °C for 30, 60, 90, and 120 min, respectively. Subsequently, the alterations in their dimensions were quantitatively assessed. It is necessary to note that the temperature range specified above falls within the sintering range of the synthesized glasses, as indicated in Fig. 3. The graphs in Fig. 4 illustrate the linear shrinkage of glasses under isothermal sintering conditions.

According to the findings presented in Fig. 4, it is evident that the shrinkage consistently rises as the sintering temperature increases across all four compositions. Additionally, it is noteworthy that the shrinkage rates remain relatively stable at each respective temperature.

Based on the Eq. (1), determination of n can be computed for every given temperature as follows:

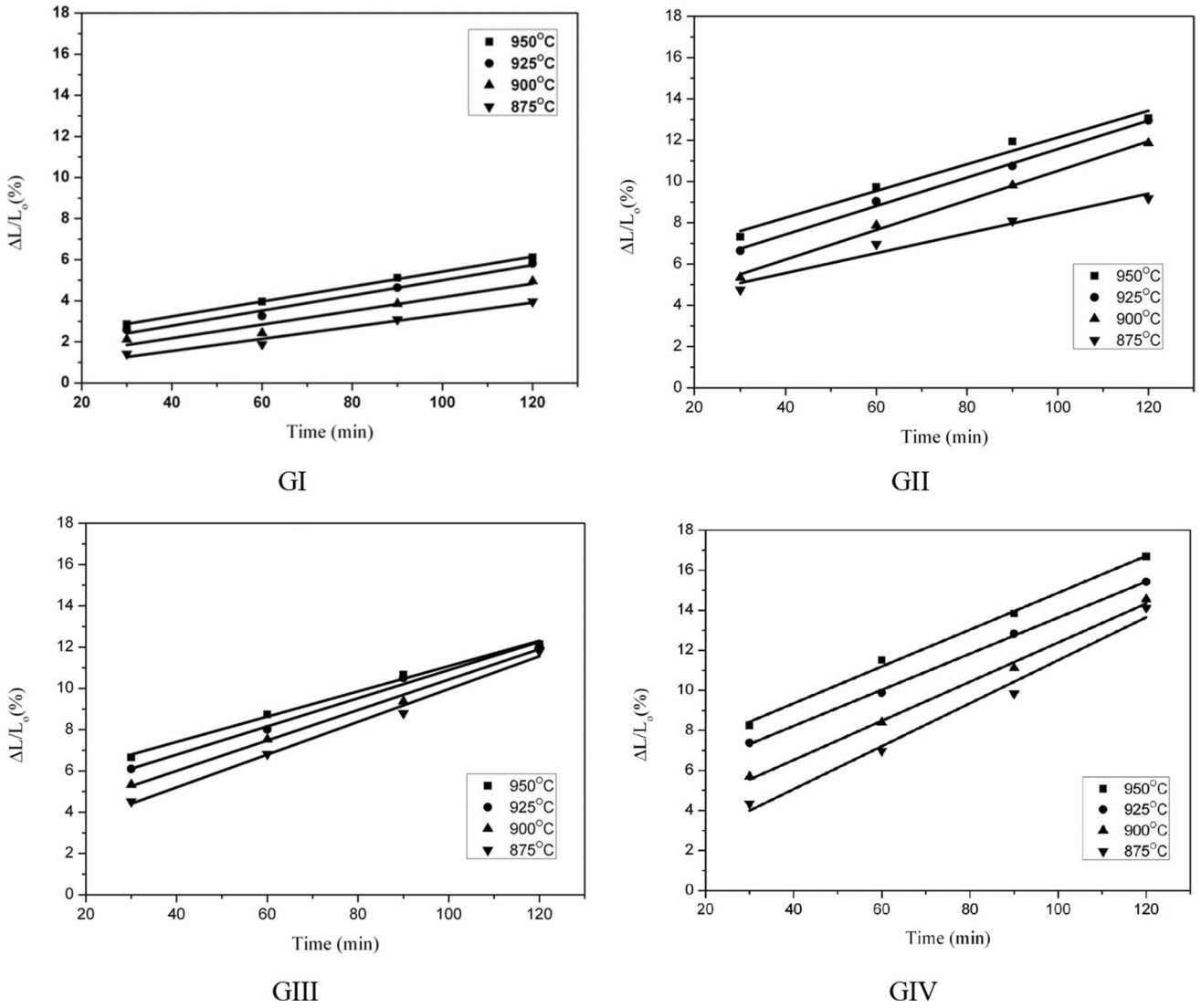

Fig. 4 Linear shrinkage of the synthesized glasses versus time at constant sintering temperature

$$n\ \mathrm{Ln}(\Delta L/L0) = \mathrm{Ln}(K/T) + \mathrm{Ln}\ t \tag{3}$$

To clarify, by plotting $\mathrm{Ln}(\Delta L/L_0)$ versus of Ln t, the resulting line will have a slope equal to 1/n. Hence, through the computation of the slope of the depicted lines at various temperature, the parameter n can be determined. Subsequently, by employing Eq. (3), the parameter K may be derived for each sintering duration and temperature. Then, by plotting Ln K_{Ave} versus of 1/T according to Eq. (2), a linear equation is acquired in which slope and y-intercept are equal to (-E/R) and $\mathrm{Ln}K_o$, respectively. Determination of the sintering activation energy can be achieved by analyzing the gradient of the lines depicted in Fig. 5. The results that were collected have been reported in Table 3.

According to the data presented in Table 3, it can be observed that the sintering activation energy for the GI composition is the lowest among the various compositions, while the GIV glass exhibits the highest value. This finding suggests that the sintering process in the GI is comparatively more facile and results in a more comprehensive consolidation compared to the other compositions. On the other hand, the composition of GIV exhibits a higher activation energy and incomplete development of sintering, which can be attributed to the processes of crystallization and viscosity increment. The agreement between the activation energy of viscous flow determined using the isothermal approach and the data derived from the sintering and density curves is confirmed.

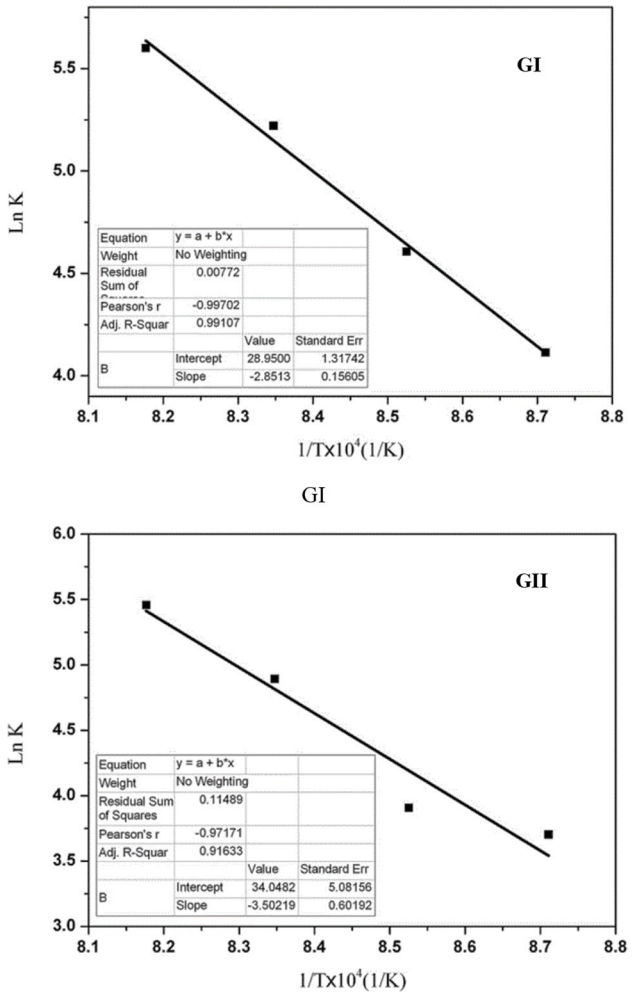

Fig. 5 Calculating the sintering activation energy of synthesized glasses

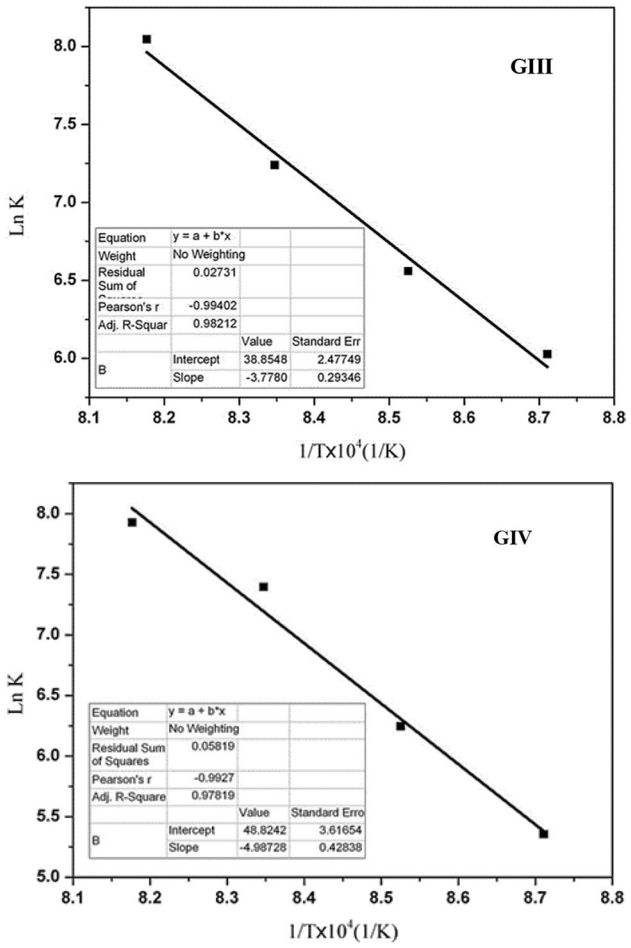

Fig. 5 (continued)

Table 3 Sintering activation energy (kJ/mol) of synthesized glasses in isothermal condition

Sintering activation energy (kJ/mol)	GI	GII	GIII	GIV
	237.05	291.15	314.10	414.64

3.3 The Sintering Activation Energy of Glasses In Non-Isothermal Condition

Simultaneously, the dilatation curves for the specimens GI and GIV was examined using hot stage microscope to determine the activation energy associated with the lowest and highest conditions observed in the isothermal data. Figure 6 illustrates the fluctuation in shrinkage as a function of temperature, considering heating rates ranging from 10 to 25 °C/min.

It is evident that in both glass compositions, the sintering initiation temperature exhibits an increase in response to the heating rate. Similarly, when a specific temperature is reached, the degree of shrinking diminishes as the rate of heating increases.

The estimation of sintering activation energy in the non-isothermal conditions was conducted using the Cheng equation [17]:

$$\mathrm{Ln}\left(v/T^2\right) = -E/RT_x \tag{4}$$

where ν, Tx, E and R refer to the heating rate, temperatures corresponding to a fixed degree of transformation, sintering activation energy and gas constant, accordingly. By plotting the variation of $\mathrm{Ln}(\nu/T^2)$ versus 1/T, the activation energy of sintering via viscos flow mechanism can be determined from the plot slope.

The obtained results for the glass with a GI composition reveal the activation energy for sintering to be 264, 288, 284, 269, and 259 kJ/mol, corresponding to shrinkage percentages of 5, 10, 15, 20, and 25%, respectively. The sintering activation energy for GIV glass is determined to be 450, 346, 171, and 78 kJ/mol for shrinkage percentages of 0.1%, 0.5%,

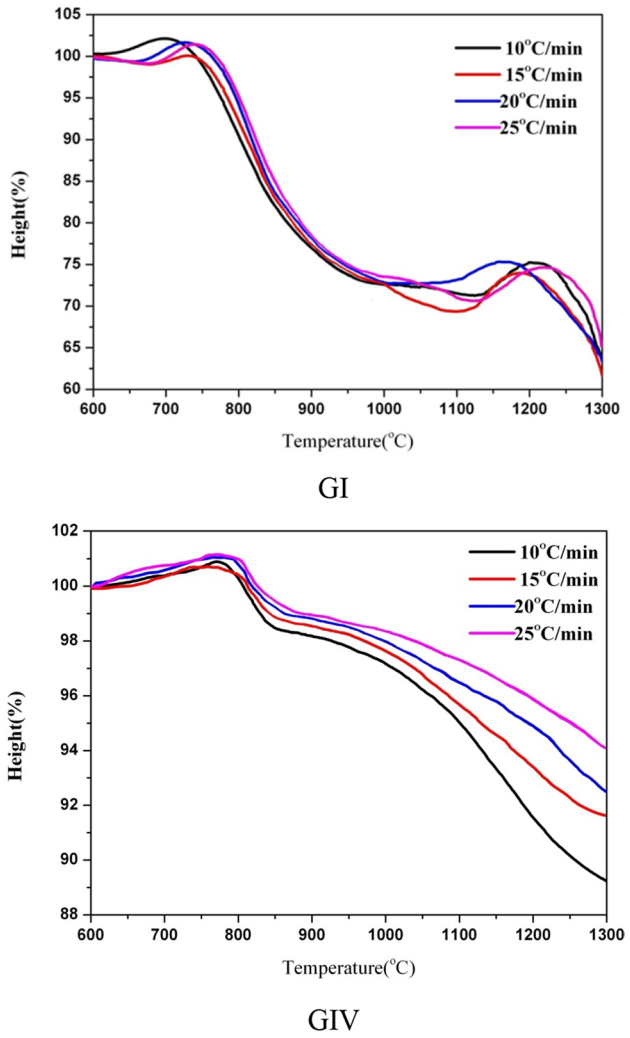

Fig. 6 shrinkage variation versus temperature of GI and GIV at non isothermal condition

Table 4 Sintering activation energy (kJ/mol) of the synthesized glasses in the non-isothermal condition

Glass	GI				
Shrinkage (%)	5	10	15	20	25
Sintering activation energy (kJ/mol)	264	288	284	269	259
Glass	GIV				
Shrinkage (%)	0.1	0.5		1	5
Sintering activation energy (kJ/mol)	450	346		171	78

1%, and 5%, respectively. The results of the calculation were summarized in Table 4.

According to Table 4, the sintering activation energy for GI exhibits minimal variation across different levels of shrinkage. Furthermore, these values are quite similar to the activation energy determined by the isothermal approach. In the context of the GIV, it has been observed that a rise in shrinkage is accompanied with a significant drop in the activation energy for sintering. As previously stated, the presence of the mullite crystal phase in this glass impedes its full sintering process. Furthermore, based on the data presented in Fig. 5, it can be inferred that the extent of shrinkage in GIV glass is influenced by the rate at which it is heated. The observed shrinkage during the heating process at a rate of 10 °C/min is around 11%, whereas at a rate of 25 °C/min, it is approximately 5%. The degree of reliance is significantly reduced in the case of GI glass, with the shrinkage levels exhibiting minimal variation across different heating rates, about amounting to 35%. Consequently, the determined values of sintering activation energy in GI glass exhibit no dependence on the extent of shrinkage.

It appears that the heating process leads to the crystallization of a substantial quantity of mullite within GIV glass. This phenomenon is observed to progressively enhance the porosity of the material, thereby resulting in a reduction in thermal conductivity. The observed behavior has resulted in an elevated reliance of the shrinkage rate on the heating rate, while concurrently decreasing the activation energy for sintering in this glass.

Given that crystallization and growth are processes that depend on time, it is anticipated that a faster heating rate will result in reduced crystallization and thus lead to increased shrinkage in the system. However, it is seen that the initiation of viscose flow occurs at a lower temperature when the rate is decreased. This can be attributed to the smaller temperature difference between the sample and the furnace, as depicted in Fig. 6. Indeed, it appears that there is a competitive relationship between the two factors involved in the glass sintering process. Specifically, in GIV glass, the primary factor influencing the process is the delay in the initiation of viscous flow at higher heating rates. Consequently, this factor assumes a determining and dominant role, resulting in a decrease in the extent of shrinkage as the heating rate increases.

4 Conclusion

Monolithic, crack-free, and transparent glasses was successfully synthesized by sintering of monolithic sol–gel derived specimens in the Al_2O_3-B_2O_3-SiO_2 system. According to the obtained results, it can be said:

The glasses displayed a relative density more than 99% after sintering at 950 °C for 2 h.

- Crystallization of mullite led to incomplete densification of the high bearing Al_2O_3 and ZnO glass.
- Under isothermal conditions, the activation energy for sintering of the glasses increased from 237 to 414 kJ/mol with variation of glass composition.

- Under non-isothermal conditions, it was observed that the sintering activation energy at various shrinkage levels of GI glass exhibited similar values. However, in the case of GIV glass, the sintering activation energy reduced as the shrinkage increased. In GIV glass, the extent of shrinkage at a given temperature was found to be more influenced by the rate of heating as compared to GI glass.

Author Contributions Sara Ahmadi: Conceptualization, Investigation, Methodology, Writing-Original draft preparation. Bijan Eftekhari Yekta: Conceptualization, Funding acquisition, Methodology, Project administration, Supervision, Writing-review and editing.

Funding The authors declare that no funds, grants, or other support were received during the preparation of this manuscript.

Data Availability The data underlying this article will be shared on reasonable request to the corresponding author.

Declarations

Competing Interests The authors declare no competing interests.

References

1. Cable M, Parker JM (1992) Blackie. Chapman and Hall, Glasgow, New York
2. Brinker CJ and Scherer GW (1990) Sol-gel science: the physics and chemistry of sol-gel processing academic press INC. NewYork
3. Chua KJ, Chou SK, Ho JC, Hawlader MNA (2002) Heat pump drying: Recent developments and future trends. Drying Technol 20(8):1579–1610
4. Scherer GW, Brinker CJ, Roth EP (1985) Sol→ gel→ glass: III. Viscous sintering. J Non-Cryst Solids 72(2):369–389
5. Chua KJ, Mujumdar AS, Chou SK (2003) Intermittent drying of bioproducts—an overview. Biores Technol 90(3):285–295
6. Brinker CJ, Roth EP, Scherer GW, Tallant DR (1985) Structural evolution during the gel to glass conversion. J Non-Cryst Solids 71(1):171–185
7. Zarzycki J (1997) Past and Present of Sol-Gel Science and Technology. J SolGel Sci Technol 8:17–22. https://doi.org/10.1023/A:1026480424495
8. Brinker CJ, Haaland DM (1983) Oxynitride glass formation from gels. J Am Ceram Soc 66(11):758–765
9. Li HP, Wang J, Stevens R (1993) The effects of hydroxide gel drying on the characteristics of co-precipitated zirconia-hafnia powders. J Mater Sci 28(2):553–560
10. Marshall WR (1953) Drying. Ind Eng Chem 45(1):47–54
11. Shih C, Pan Z, McHugh T, Wood D, Hirschberg E (2008) Sequential infrared radiation and freeze-drying method for producing crispy strawberries. Trans ASAE (Am Soc Agric Eng) 51(1):205
12. Ahmadi S, EftekhariYekta B, Sarpoolaky H, Aghaei A (2022) Preparation of Monolithic Transparent Mullite- Based Glass-Ceramics by the Sol- Gel Method. J Non-Cryst Solids 575:121186
13. Ahmadi S, Eftekhari Yekta B, Sarpoolaky H, Aghaei A (2021) Physical and structural characteristics of gel-derived glasses prepared via different drying procedures. IJMSE 18(4):1–9
14 EftekhariYekta B, Marghussian VK (1999) Sintering of β.q.ss. and gahnite glass-ceramic/silicon carbide composites. J Eur Ceram Soc 19(16):2969–2973
15. Brinker EPRCJ, Scherer GW (1985) Sol-Gel-Glass:physical and structural evolution during constant heating rate experiments. J Non-Cryst Solids 72:345–368
16. Jean J-H, Gupta TK (1992) Isothermal and nonisothermal sintering kinetics of glass-filled ceramics. J Mater Res 7(12):3342–3347
17. Karamanov A, Dzhantov B, Paganelli M, Sighinolfi D (2013) Glass transition temperature and activation energy of sintering by optical dilatometry. Thermochim Acta 553:1–7

Publisher's Note Springer Nature remains neutral with regard to jurisdictional claims in published maps and institutional affiliations.

Springer Nature or its licensor (e.g. a society or other partner) holds exclusive rights to this article under a publishing agreement with the author(s) or other rightsholder(s); author self-archiving of the accepted manuscript version of this article is solely governed by the terms of such publishing agreement and applicable law.